COMBINED ELECTRICAL AND MECHANICAL COUPLING FOR MODE-RECONFIGURABLE CMOS-MEMS FILTERS

Chao-Yu Chen[1], Ming-Huang Li[1], Chi-Hang Chin[1], Cheng-Syun Li[1], and Sheng-Shian Li[1,2]
[1]Institute of NanoEngineering and MicroSystems, [2]Department of Power Mechanical Engineering
National Tsing Hua University, Hsinchu, Taiwan

ABSTRACT

This work presents a novel filter scheme which combines both electrical and mechanical coupling mechanisms implemented in a CMOS-MEMS filter to simultaneously attain small percent bandwidth through weakly mechanical link and decent stopband rejection via differentially electrical configuration. As compared to the traditional parallel-class (i.e., electrically-coupled) filters and mechanically-coupled filters, the proposed oxide-rich filter structure features flexible electrical routing and non-conductive mechanical filter couplers, hence enabling common-mode to differential (CIDO) and differential to common-mode (DICO) reconfigurable modes all within a single device. The proposed 8.6-MHz CMOS-MEMS filter has been successfully demonstrated with a narrow passband of 35 kHz (0.41% bandwidth) and stopband rejection more than 20 dB under proper termination.

INTRODUCTION

To meet the demand of miniaturization for modern wireless communication systems and sensor networks, the low-power and compact transceivers play an important role from the Internet of Things (IoT) to smart life for human beings. However, a few discrete mechanical transducers, such as reference oscillators (e.g., quartz) and band-select filters (e.g., SAW), in current front-end communication systems are still necessitated, thus impeding the trend toward on-chip integrated transceivers. To address this issue, the MEMS oscillators [1][2] and filters [3]-[6] have been intensively studied in the past decade, so far realizing small form factor and bringing cost-effective and robust features to replace their bulky counterparts abovementioned. Although the MEMS-based devices greatly reduce the RF front-end chip area as in [7], the additional wire-bonding or packaging technology (e.g., TSV) is still necessary to form electrical connections between the MEMS devices and CMOS circuits (i.e., system in package, SiP), therefore hindering the single chip solution in the future.

On the other hand, CMOS-MEMS platforms [8] take advantage of the existing layers in CMOS back-end-of-line (BEOL) to fabricate the mechanical devices. Through the standard CMOS foundry processes, the MEMS resonators feature not only high Q and small footprint, but integration with ICs. The CMOS-MEMS filters to date are designed into two main categories, including electrically-coupled [9][10] and mechanically-coupled [11][12] filter topologies. The electrically-coupled design can easily achieve a narrow filter passband using two or more resonator output signals coupled by an additional readout circuit (e.g., TIA or Buffer).

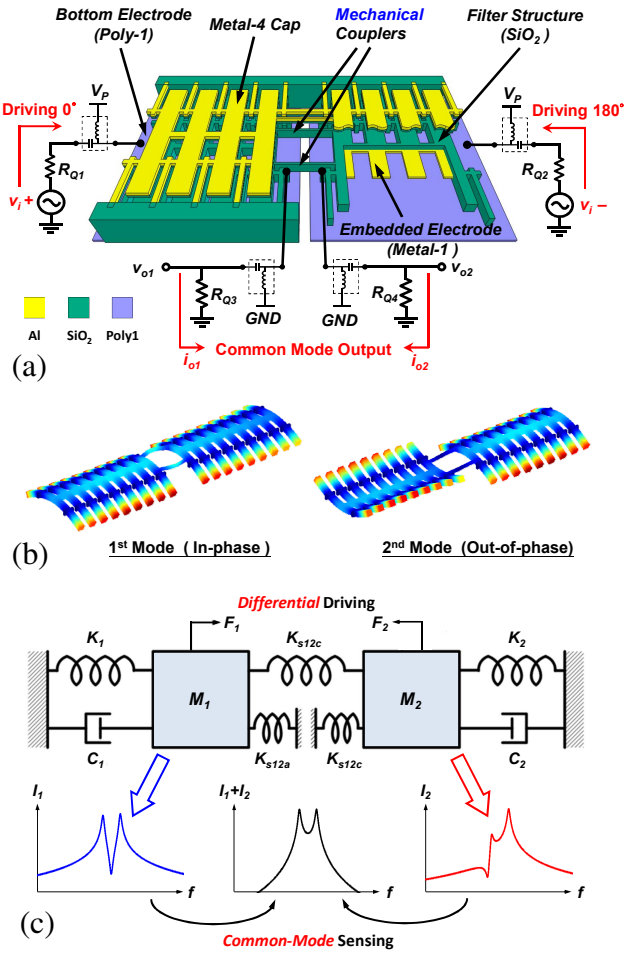

Fig. 1: (a) Perspective-view schematic, (b) finite element simulation of the proposed filter structure and (c) qualitative description of the equivalent model for the proposed filter in a differential to common-mode (DICO) configuration.

However, the use of extra circuits may lead to more power consumption; in addition, the process variation of resonators would cause frequency discrepancy, resulting in large in-band ripples of the filter. On the contrary, the filter bandwidth of mechanically-coupled filters is well defined through the physical filter coupler but very difficult to suppress the background feedthrough signals from the substrate under a typical two-port configuration.

In this work, we propose a novel coupling concept which combines electrically and mechanically-coupled mechanisms together for narrow-bandwidth filter implementation. Based on the thorough modeling of capacitive transducers [13], the

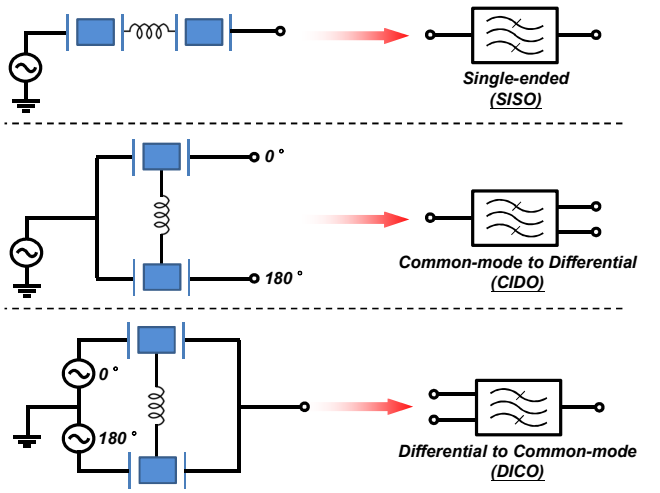

Fig. 2: Concept of the mode-reconfigurable CMOS-MEMS filter.

arraying design [12] and deep submicron gap process [14] are adopted in the proposed filter to take advantage of the low motional impedance (R_m) resonant tanks. Moreover, two weak filter couplers close to nodal locations of the constituent resonators (i.e., low-velocity coupling) together with a differentially operating configuration facilitate the filter termination, thus resulting in flat passband and decent stopband rejection. By using the proposed concept, the CMOS-MEMS filter structure enables the operation of (i) single-ended (SISO), (ii) common-mode to differential (CIDO), and (iii) differential to common-mode (DICO) configurations in a single device, paving a way for the future filter implementation.

CMOS-MEMS FILTER DESIGN

Fig. 1(a) presents the perspective view schematic of the proposed filter operated in a differential to common-mode (DICO) configuration (one of the implementations). The oxide-rich filter structure is composed of two free-free beam (FFB) resonator arrays mechanically linked by two flexural filter couplers close to the nodal locations of the vibrating FFBs to enable narrow passband (i.e., low velocity coupling scheme [13]). Notably, the oxide-rich structure [15] and mechanically arrayed design would provide higher quality factor (Q) than its metal-alloy counterpart [12] and simultaneously increase the effective transduction areas, thus evidently reducing the insertion loss (*I.L.*) of the filter.

Unlike the traditional mechanically-coupled filters operating in a two-port biasing and excitation configuration (SISO), a differentially driving signals (v_i+ and v_i-) together with a dc bias (V_P) are applied onto the bottom poly-Si electrodes (Poly-1) to concurrently drive the filter structure into vibration with two physical mode shapes shown in the Fig. 1(b). The common-mode output current can then be sensed by the embedded electrodes (Metal-1) inside the SiO_2 filter structure. To understand the working principle, Fig. 1(c) illustrates the transfer function plots of the proposed filter based on a DICO configuration. In this system, the

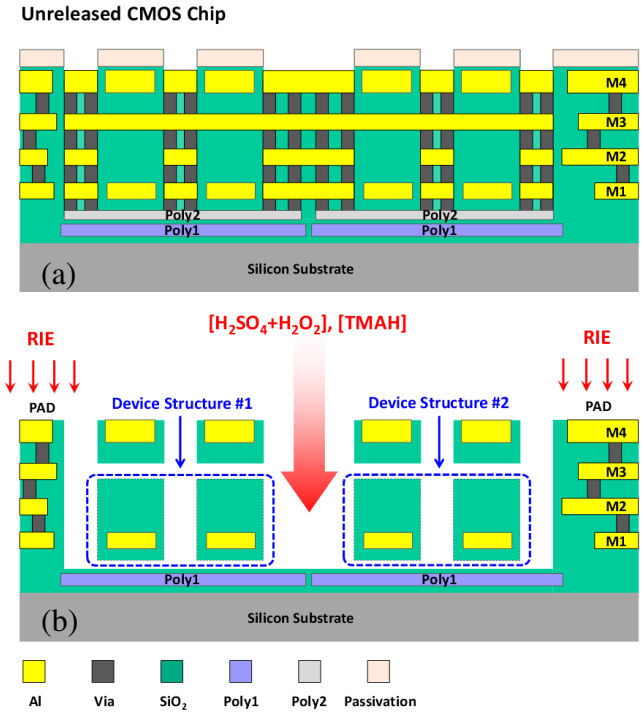

Fig. 3: Cross-sectional view of the CMOS-MEMS filter (a) before and (b) after post-CMOS processing. Note that the device structure #1 and #2 are electrically isolated, due to non-conductive couplers.

motional current (I_i) can be individually detected from a single resonant unit, given by

$$I_i = \eta_e (j\omega X_i) \quad (1)$$

where X_i is the displacement of a single resonant tank; i numbers each resonant tank of the filter (i= 1, 2); and η_e is the electromechanical coupling factor of the capacitive transducer. The desirable filter spectrum (I_1+I_2) is formed by summing the motional signals I_1 and I_2 together. By the use of the differential operation, the undesired parasitic feedthrough signals can be effectively eliminated. Therefore, this topology features evident improvement on noise floor without the use of any de-embedding technique as compared to our previous work [12].

Moreover, the proposed filter is also capable of realizing various configurations as different electrical setups are carried out, such as (i) a traditional mechanically-coupled filter (single-ended, SISO) operated in a typical two-port configuration and (ii) a common-mode to differential filter (CIDO), respectively, as depicted in Fig. 2. With this flexibility, the designer can freely chose the operation conditions dependent on the system requirements. Furthermore, the feature of the unique port reconfigurable capability (i.e., CIDO and DICO) physically realizes an on-chip single-to-balance converter without any discrete balun transformer, facilitating the implementation of a miniaturized, integrated transceiver.

FABRICATION PROCESS

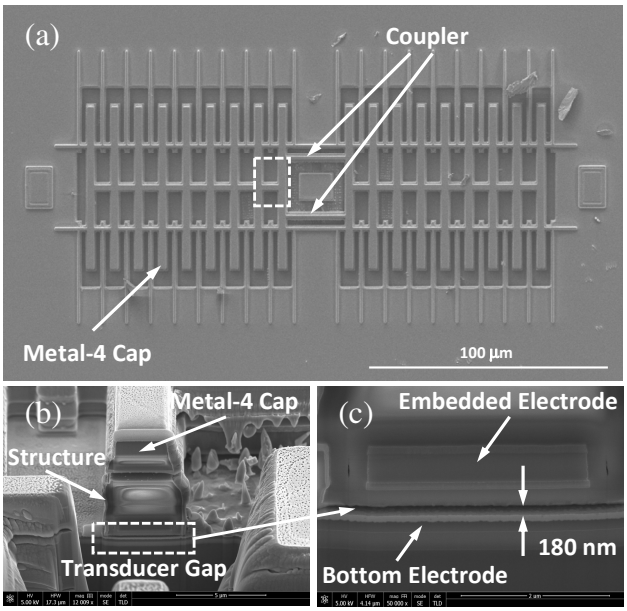

Fig. 4: SEM pictures of the proposed CMOS-MEMS filter: (a) the global view, (b) cross-section of a free-free beam structure, and (c) transducer's gap-zoomed view.

As aforementioned, the oxide-rich filter is fabricated using a standard foundry-oriented CMOS-MEMS platform [14]. Fig. 3 indicates the cross-sectional view and post-CMOS process flow for the proposed CMOS-MEMS filter. To well define the structure profile, a two-step wet etching process [14] is adopted in this work for achieving the tiny transducer's gap without the special structure design (i.e., pull-in frame designed in [12]). First, a metal etchant composed of sulfuric acid (H_2SO_4) and hydrogen peroxide (H_2O_2) is utilized to remove the sacrificial metal layer under the passivation-free region due to the high selectivity to SiO_2. Then a TMAH wet etching is used to remove the exposed polysilicon layer (Poly-2) for realizing deep submicron gap spacing. Note that the top Metal-4 cap serves to protect the device structure during the final RIE pad-opening process.

After the maskless release process, Fig. 4(a) presents a global SEM view of the fabricated CMOS-MEMS filter on which the metal protection layer (Metal-4 Cap) is clearly seen. Fig. 4(b) further shows the cross-sectional view from a focused ion beam (FIB) cut area indicated in Fig. 4(a) while a zoom-in of the transducer's gap (around 180 nm) can be easily seen in Fig. 4(c).

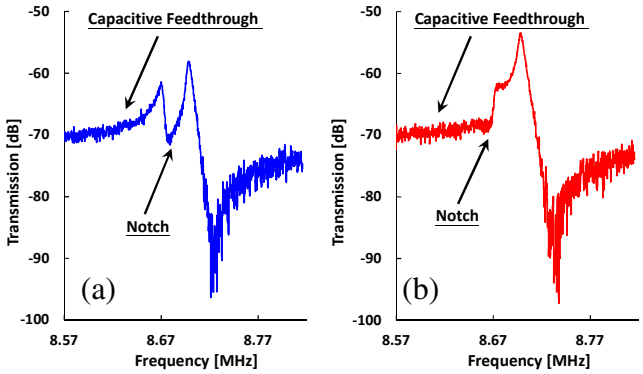

Fig. 5: CMOS-MEMS filter under a differential driving scheme while the output signals are individually accessed from (a) device structure #1 and (b) device structure #2 (denoted in Fig. 3(b)). The measured frequency characteristics match quite well with the theoretical prediction (cf. Fig. 1(c)).

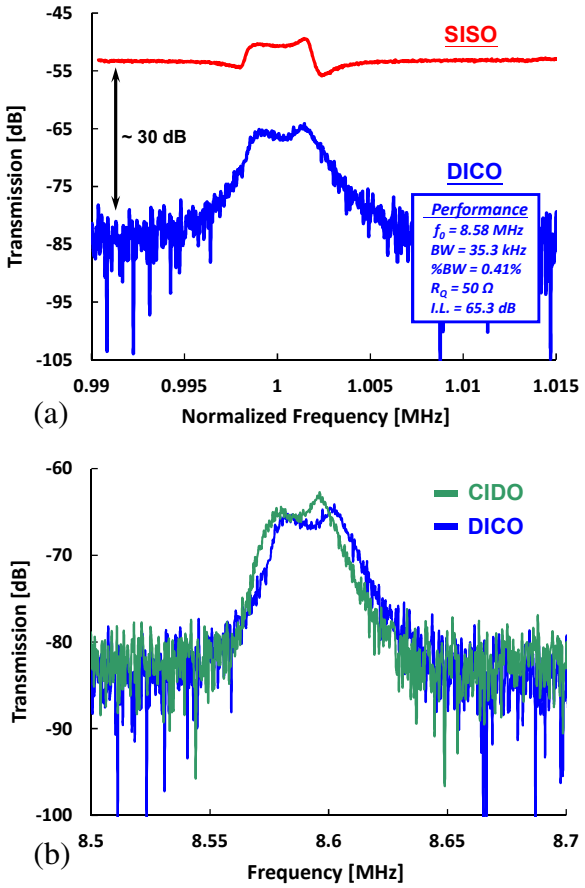

Fig. 6: Comparison of the transmission spectra: (a) SISO vs. DICO operation, and (b) CIDO vs. DICO operation.

MEASUREMENT RESULTS

To verify the performance of the DICO configuration illustrated in Fig. 1(c), the fabricated filters are tested under a 1 mTorr environment using a cryogenic vacuum chamber with a proper bias voltage (around 60 V). Since the non-conductive filter couplers are used to connect two distinct resonant tanks, we can drive this filter into resonance through differential signals while individually accessing output signals from different parts of the filter structure (i.e., #1 and #2 denoted in Fig. 3(b)) with the measured spectra shown in Fig. 5(a) and (b), respectively. However, the measured transmission exhibits some discrepancy in background feedthrough level as compared to an ideal simulation (cf. Fig. 1(c)) due to the existence of undesired feedthrough capacitance (C_f) coupling from the substrate, but still in good agreement with our theoretical prediction in (1).

As abovementioned, the proposed filter is capable of operating in various configurations. Fig. 6(a) and (b) successfully demonstrate the mode-reconfigurable capability

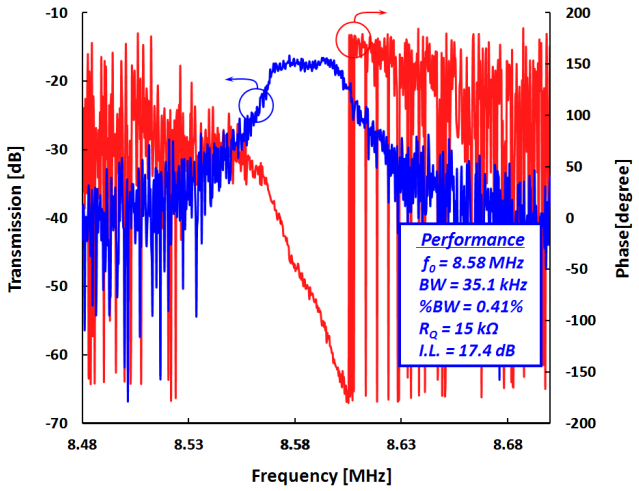

Fig. 7: Terminated frequency spectrum of the CMOS-MEMS filter in a DISO configuration.

in a single device. Notably, as compared to the conventional mechanically-coupled filter operated in SISO setup, the differential configuration provides feedthrough cancellation that creates a 30-dB improvement on the feedthrough floor as shown in Fig. 6(a). In addition, there is no difference on bandwidth between SISO and DICO operation, implying that the filter bandwidth is preserved and determined by the geometry design and location of the filter couplers. Also, the comparison of CIDO and DICO configurations is provided in Fig. 6(b) where the filter spectra show very similar performance in terms of transmission magnitude and bandwidth. Note the deviation of the filter center frequency is mainly caused by different diving conditions.

Fig. 7 finally presents a terminated spectrum and phase transition for the 8.6-MHz CMOS-MEMS filter under a DICO configuration with the stopband rejection greater than 20 dB thanks to the differential operation. As a result, the flatten passband is attained with a narrow 0.41% bandwidth and insertion loss of 17.4 dB when the port resistance (R_Q) of 15 kΩ is adopted in the termination network.

CONCLUSIONS

In this work, we demonstrate the micromechanical filter fabricated by a foundry-orientation CMOS-MEMS platform. To attain low-loss and channel-select features, the high-Q structural material (i.e., silicon dioxide) and beam-arrayed resonator design are implemented in the proposed filter. Moreover, the combination of metal and polysilicon etching processes is adopted for the post-CMOS release to create deep submicron transducer's gap to further reduce the motion impedance. Finally, the novel concept combining electrical and mechanical coupling for future multi-mode systems is reported in this work. By employing this topology, various operating configurations can easily be realized in a single device. As a result, the proposed filter demonstrates a narrow percent bandwidth (0.41%) and acceptable stopband rejection benefiting from the precise coupler design and differential operation.

ACKNOWLEDGEMENTS

The author would like to thank the supported by the National Science Council (NSC) of Taiwan under grant of NSC-101-2628-E-007-008-MY2, also appreciate the TSMC and National Chip Implementation Center (CIC), Taiwan, for the device manufacturing and CAD tools providing.

REFERENCES

[1] Y.-W. Lin, *et al.*, "Series-resonant VHF micromechanical resonator reference oscillators," *IEEE J. Solid-State Circuits*, vol. 39, no. 12, pp. 2477-2491, 2004.

[2] C. T.-C. Nguyen, "MEMS technology for timing and frequency control," *IEEE Trans. Ultrason., Ferroelect., Freq. Contr.*, vol. 54, no. 2, pp. 251-270, 2007.

[3] S. Pourkamali, *et al.*, "Electrically coupled MEMS bandpass filters part II. Without coupling elements," *Sensors and Actuators A*, vol. 122, pp. 317-325, 2005.

[4] D. Weinstein, *et al.*, "Dielectrically transduced single-ended to differential MEMS filter," *Dig. ISSCC'06*, pp. 318-319, 2006.

[5] S.-S. Li, *et al.*, "An MSI micromechanical differential disk-array filter," *Dig. Transducers'07*, pp. 307-311, 2007.

[6] S. Wang, *et al.*, "Encapsulated mechanically coupled fully-differential breathe-mode ring filters with ultra-narrow bandwidth," *Dig. Transducers'11*, pp. 942-945, 2011.

[7] A. Heragu, *et al.*, "A 2.4 GHz MEMS based sub-sampling receiver front-end with low power channel selection filtering at RF," *IEEE RFIC'12*, pp. 257-260, 2012.

[8] W.-C. Chen, *et al.*, "A generalized CMOS-MEMS platform for micromechanical resonators monolithically integrated with circuits," *J. Micromech. Microeng.*, vol. 21, no. 6, pp. 065012, May 2011.

[9] J. Lopez, *et al.*, "A CMOS–MEMS RF-tunable bandpass flter based on two high-Q 22-MHz poly-silicon clamped-clamped beam resonators," *IEEE Electron Device Lett.*, vol. 30, no. 7, July 2009.

[10] J Giner, *et al.*, "A fully integrated programmable dual-band RF filter based on electrically and mechanically coupled CMOS-MEMS resonators," *J. Micromech. Microeng.*, vol. 22, no. 5, 055020 (6pp), April 2012.

[11] J. Giner, *et al.*, "A CMOS-MEMS filter using a v-coupler and electrical phase inversion," *IEEE IFCS10,* pp. 344-348, 2010.

[12] C.-Y. Chen, *et al.*, "Design and characterization of mechanically-coupled CMOS-MEMS filters," *Dig. Transducers'13*, pp. 2288-2291, 2013.

[13] F. D. Bannon III, *et al.*, "High-Q HF microelectromechanical filters," *IEEE J. Solid-State Circuits*, vol. 35, no. 4, pp. 512-526, 2000.

[14] C.-H. Chin, *et al.*, "A CMOS-MEMS resonant gate field effect transistor," *Dig. Transducers'13*, pp. 2284-2287, 2013.

[15] W.-C. Chen, *et al.*, "VHF CMOS-MEMS oxide resonators with Q > 10,000," *IEEE IFCS12,* pp. 1-4, 2012.

CONTACT

* S.-S. Li, Tel: +886-3-516-2401; ssli@mx.nthu.edu.tw